

2D- π -A Type Organic Dyes Based on *N,N*-Dimethylaryl Amine and Rhodamine-3-acetic Acid for Dye-sensitized Solar Cells

Tang, Kai^a(唐恺) Liang, Mao^b(梁茂) Liu, Yongkang^a(刘永康)
Sun, Zhe^b(孙喆) Xue, Song^{*b}(薛松)

^a Department of Chemistry, University of Science and Technology of China, Hefei, Anhui 230026, China

^b Department of Applied Chemistry, Tianjin University of Technology, Tianjin 300384, China

Three organic dyes **XS17**–**19** based on *N,N*-dimethylaryl amine and rhodamine-3-acetic acid moieties are designed and synthesized. These dyes were applied into nanocrystalline TiO₂ dye-sensitized solar cells through standard operations, showing strong absorption bands at around 320–650 nm, and exhibiting broad IPCE responses. Cell based on **XS17** gave a J_{sc} of 3.7 mA/cm², an open circuit voltage of 550 mV, and a fill factor of 0.68, corresponding to an overall conversion efficiency of 1.4%. The low overall conversion efficiency is due to the modest IPCE and V_{oc} values, which mainly stem from the acceptor of rhodamine-3-acetic acid.

Keywords dye-sensitized solar cell, photovoltaic, *N,N*-dimethylaryl amine, organic dyes

Introduction

Dye-sensitized solar cells (DSSCs), which emerged as a new generation photovoltaic device, have received considerable attention in recent years because of their high efficiency and low-cost since 1991.¹ In these components, dye is one of the key components for high power conversion efficiencies. Until now, two kinds of sensitizer, metal-organic complexes^{2,3} and metal-free organic dyes,^{4–19} were developed for light harvesting. It is of great interest to design and synthesize metal-free organic dyes, owing to their high molar absorption coefficient, simple synthesis procedure and high efficiency, although Ru complexes have achieved power conversion efficiencies over 11% under AM 1.5 irradiation.²⁰ Recently, organic dyes used for the DSSCs were developed rapidly, which indicated the promising perspective of organic dyes for cells. Great effort has been made on the design of new organic dyes in order to obtain excellent sensitizers with high power conversion efficiency and long-term stability.

Most organic sensitizers are constituted by donor, conjugate bridge, and acceptor moieties, thereby forming a D- π -A structure. Recently, organic dyes with 2D- π -A structure are reported by several groups.^{21–23} Their studies suggested that good performance of organic dyes based on 2D- π -A structure over the simple D- π -A configuration could be achieved by molecular design. The double donor moieties afforded organic sensitizers with high electron-density of donor, which resulted in enhanced molar extinction coefficient and high overall power conversion efficiency.²⁴

Based on the above consideration, we have designed and synthesized three new organic sensitizers **XS17**–**19** (Scheme 1), which consist of double *N,N*-dimethylaryl amine moieties as electron-donating groups, as well as diphenylvinyl moieties, which is a possible alternative to induce a red shift of the absorption spectrum and to retain efficient light-induced charge separation. Meanwhile, the thiophene and phenyl units act as π -bridge to adjust the molecular energy levels of the dyes, and rhodamine-3-acetic acid acts as electron acceptor. Here, we wish to report the synthesis, characterization, and photovoltaic properties of these new organic dyes.

Results and discussion

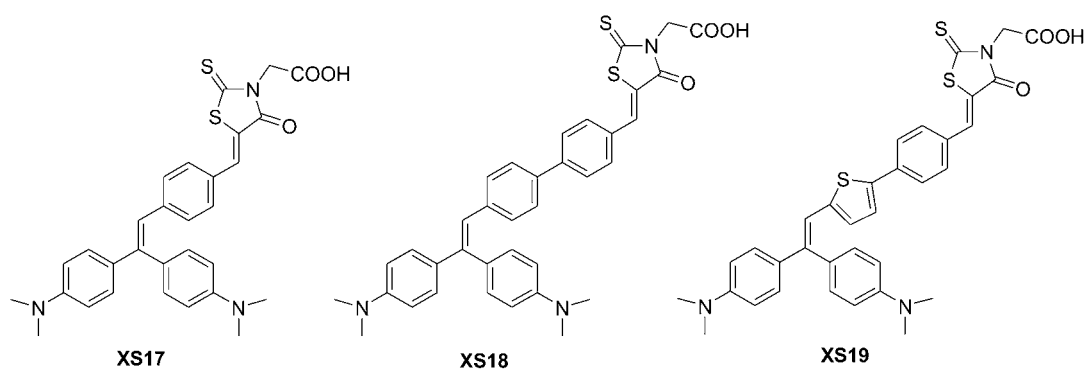
The synthetic routes of the organic dyes **XS17**–**19** are shown in Scheme 2. Treatment of compound **1** with *n*-BuLi and DMF gave an aldehyde **2**. The target dye **XS17** was obtained via Knoevenagel condensation reaction of the aldehyde **2** with rhodamine-3-acetic acid in the presence of a catalytic amount of piperidine. The aldehyde **4** was prepared from boronic acid **3** and 4-bromobenzaldehyde via Suzuki coupling reaction. Treatment of phosphonate **5** with thiophene-2-carbaldehyde in the presence of *t*-BuOK gave intermediate **6**. Aldehyde **7** was prepared from **6** via bromination reaction with NBS and Suzuki reaction with 4-formylphenylboronic acid. Subsequently, the Knoevenagel condensation reactions of aldehydes **4** and **7** with rhodamine-3-acetic acid gave the target dyes **XS18** and **XS19**, respectively.

* E-mail: xuesong@ustc.edu.cn

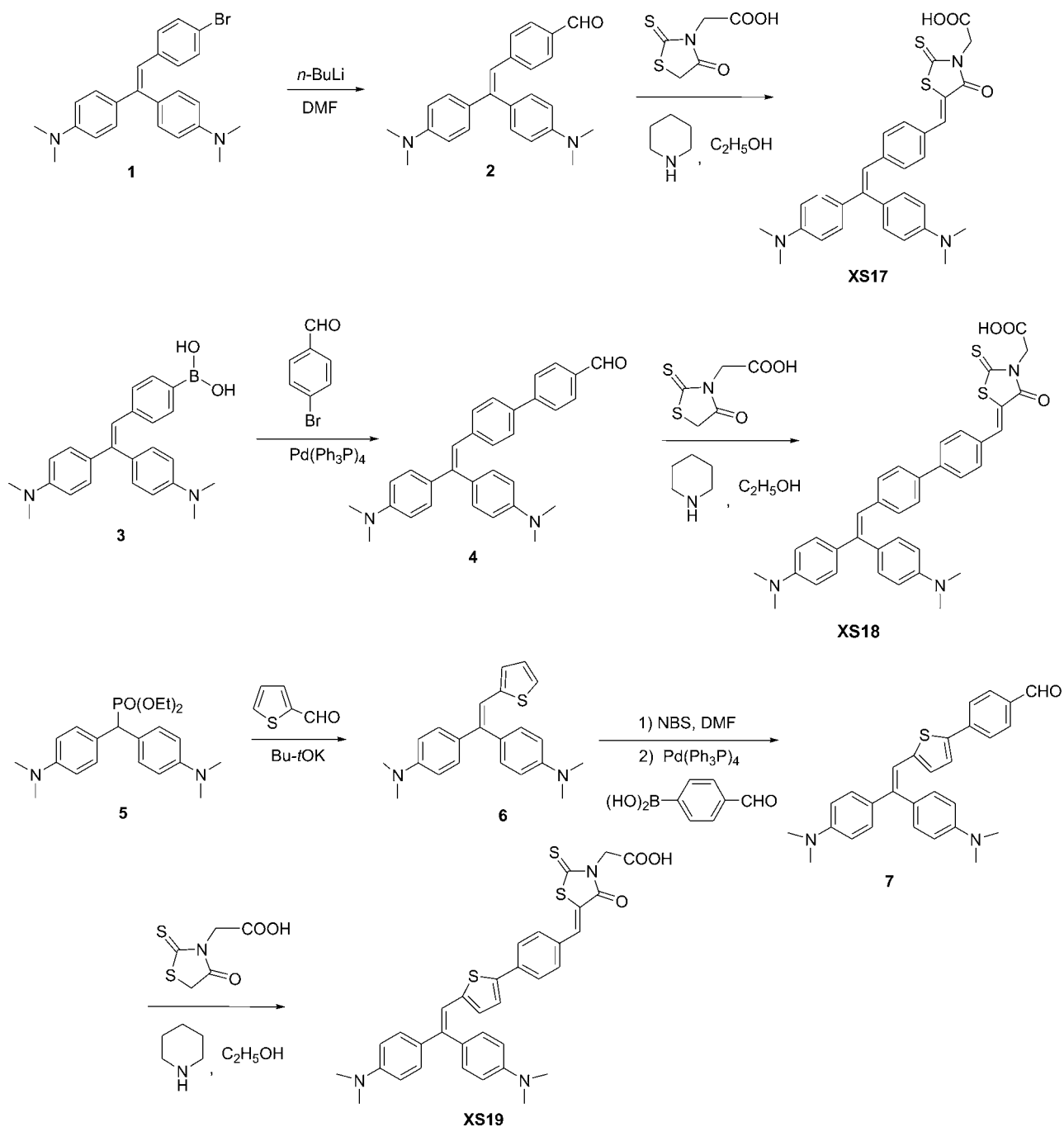
Received June 29, 2010; revised August 31, 2010; accepted September 24, 2010.

Project supported by the National 863 Program (No. 2009AA05Z421) and the Tianjin Natural Science Foundation (No. 09JCZDJC24400).

Scheme 1 Structure of dyes XS17–19



Scheme 2 Synthesis of organic dyes XS17–19



The UV-vis and emission spectra of organic dyes in chloroform solution are listed in Table 1. As shown in Figure 1, the three dyes **XS17**–**19** show strong absorption bands at around 320–650 nm, and display two visible bands, appearing at 374/500 nm, 388/444 nm and 394/496 nm, respectively. The first absorption bands for three dyes are similar, which are attributed to the π - π^* electron transition of the conjugated molecule.²⁵ However, the second absorption bands for three dyes are obviously different from each other. To gain insight into this optical properties, time-dependent DFT (TDDFT) calculations of the excited states were performed on the optimized model at the B3LYP/6-31G(d) level *in vacuo*. The lowest 10 singlet-singlet electronic transitions are calculated and the electronic states with the largest oscillator strength (f) for the **XS17**–**19** dyes are HOMO→LUMO ($f=0.78$, 2.22 eV), HOMO–2→LUMO ($f=1.35$, 2.98 eV) and HOMO→LUMO ($f=0.94$, 1.99 eV), respectively. The isodensity surface plots of them are presented in Figure 2. For the **XS17** and **XS19**, the HOMO is delocalized on the diphenylethene and phenyl; the LUMO is, on the other hand, delocalized across the phenyl and rhodamine group, with sizable contributions from the latter. The second absorption band for **XS17** and **XS19** can be considered as an intramolecular charge transfer (ICT) transition excitation from HOMO to LUMO.²⁶ In contrast, the second absorption band for **XS18** is significantly blue-shifted compared to the **XS17** and **XS19**. It can be seen from the electronic states mentioned above as well. The HOMO–2 of **XS18** is delocalized throughout the entire molecule, with maximum components on the two phenyl rings that lies between rhodamine and diphenylethene; the LUMO is a single π^* orbital delocalized across the phenyl and rhodamine group, with similar contribution from the latter. The second absorption band for **XS18** might stem from the π - π^* transition from HOMO–2→LUMO. This excited energy of π - π^* transition is higher than that of ICT transition for

Table 1 Optical properties and electrochemical properties of the three dyes

Dye	$\lambda_{\max}^a/\text{nm}$ [$\epsilon/(\text{L}\cdot\text{mol}^{-1}\cdot\text{cm}^{-1})$]	$\lambda_{\max}^b/\text{nm}$	$\lambda_{\text{int}}^c/\text{nm}$	E_{0-0}^d/eV	$E_{\text{ox}}^e/\text{V vs. NHE}$	$E_{\text{red}}^f/\text{V vs. NHE}$
XS17	374 (23875), 500 (37408)	655	583	2.12	0.88	–1.24
XS18	388 (52852), 444 (37004)	565	514	2.41	0.84	–1.57
XS19	394 (32224), 496 (21104)	621	551	2.25	0.82	–1.43

^a Absorption spectra, ^b emission spectrum. ^c The intersect of the normalized absorption and the emission spectra. ^d E_{0-0} values were calculated from intersect of the normalized absorption and the emission spectra (λ_{int}): $E_{0-0}=1240/\lambda_{\text{int}}$. ^e The oxidation potentials (vs. NHE) of dyes were measured in CH_3CN with tetrabutylammonium perchlorate (TBAP, 0.1 mol/L) as supporting electrolyte. ^f E_{red} was calculated from $E_{\text{ox}}-E_{0-0}$.

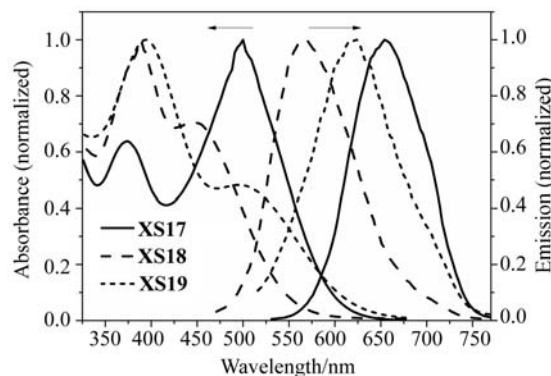


Figure 1 Absorption and emission spectra of dyes **XS17**–**19** in chloroform (5×10^{-5} mol/L).

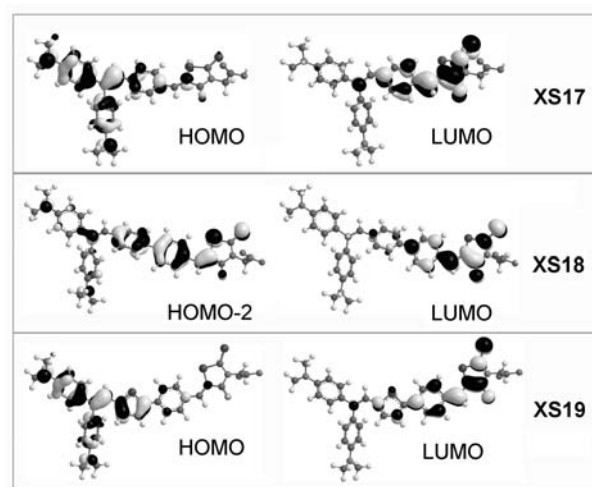


Figure 2 Isodensity surface plots of the HOMO and LUMO of **XS17**–**19**.

XS17 and **XS19**, consequently, resulting in the blue shift of the second absorption band for **XS18**. Interestingly, according to the experimental absorption of **XS17**–**19**, the ICT transition process are in the order of **XS17**>**XS19**>**XS18**. Theoretical calculation suggests that the ICT transition of **XS17**–**19** is dependent on the molecular geometry. The spacer in **XS17** is shorter than that of **XS18**–**19**, leading to an effective ICT transition from the diphenylethene to rhodamine ring. In contrast, the spacer for **XS18**–**19** is too large for an effective ICT transition. The only difference for **XS18**–**19** is π spacer, the former contains two phenyl units, the latter contains a thiophene unit and a phenyl unit. The dihedral angles of them are 43.4° and 22.0° , respectively. Therefore, **XS19** gave a more planar conjugating system compared to **XS18** because of the smaller torsion angle,²⁷ and favored the ICT transition.

It is found that the molar extinction coefficients (ϵ) of three dyes ($21104 \text{ L}\cdot\text{mol}^{-1}\cdot\text{cm}^{-1}$ to $37408 \text{ L}\cdot\text{mol}^{-1}\cdot\text{cm}^{-1}$) are much higher than that of ruthenium complexes, (**N719** dye, $14100 \text{ L}\cdot\text{mol}^{-1}\cdot\text{cm}^{-1}$), indicating good ability for light harvesting. Figure 3 shows the absorption spectra of **XS17**–**19** anchored on transparent mesoporous TiO_2 films ($2 \mu\text{m}$). The maximum

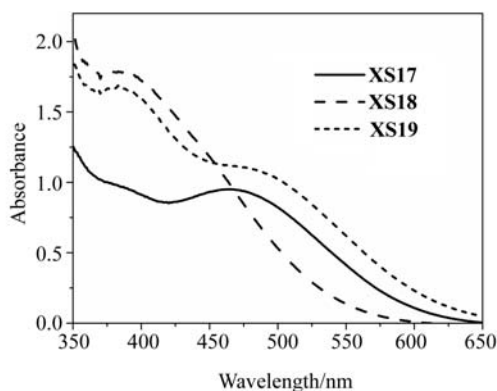


Figure 3 Absorption spectra of dyes **XS17–19** on TiO_2 film.

absorption peaks are similar to the spectra of these dyes in dichloromethane, but exhibit a slightly blue-shifted and broad absorption compared to that in solution, which may be ascribed to the formation of dye H-aggregates on the TiO_2 surface and/or the interaction between the dyes and TiO_2 .²⁸ When the dyes were excited within respective π - π^* bands in an air-equilibrated chloroform solution at 298 K, they exhibited strong luminescence maximum of 450–750 nm.

The oxidation potential (E_{ox}) of as-synthesized dyes was determined from square-wave voltammograms under Ar atmosphere. The E_{ox} corresponds to the highest occupied molecular orbital (HOMO). The reduction potential (E_{red}), which corresponds to the lowest unoccupied molecular orbital (LUMO), can be calculated from $E_{\text{ox}} - E_{0-0}$ (E_{0-0} values were calculated from λ_{int} : $E_{0-0} = 1240/\lambda_{\text{int}}$).¹³ As depicted in Figure 4, extension of the conjugation length by adding thiophene unit or phenyl unit adjusts the HOMO and the LUMO level of these dyes. Negative shifts of the HOMO level (0.04 V) and the LUMO level (0.33 V) can be observed for **XS18** vs **XS17**, which broads the HOMO and LUMO gaps. Also, this tendency holds for **XS19** vs. **XS17** due to the extension of conjugation system by introduction of thiophene unit. The LUMO levels for these dyes (−1.23 to −1.57 eV) are more negative than the conduction band of TiO_2 (−0.5 V vs. NHE), which will

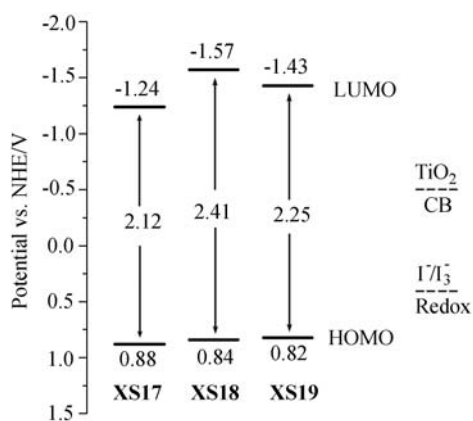


Figure 4 Schematic energy levels of **XS17–19** based on absorption and electrochemical data.

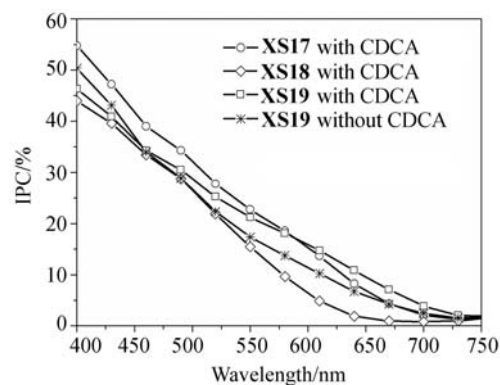


Figure 5 IPCE spectra for DSSCs based on **XS17–19**.

provide sufficient driving forces for electron injection. On the other hand, the HOMO levels for these dyes (0.82 to 0.88 eV) are more positive than the iodine redox potential (0.4 V vs. NHE).²⁹ Thus, these oxidized dyes can be regenerated from the reduced species in the electrolyte to give an efficient charge separation.

The incident photon-to-current conversion efficiency (IPCE) of DSSCs based on **XS17–19** is measured in the visible region (400–800 nm), as shown in Figure 5. To prevent dye aggregation, 3 mmol/L chenodeoxycholic acid (CDCA) was employed as a co-adsorbate. The onsets of the IPCE spectra for the dye-based devices are significantly broadened and red-shifted compared to the absorption spectrum of the dyes absorbed on TiO_2 .^{9,30} **XS17** gives a higher IPCE value between 400 nm and 800 nm than the other two dyes in this series, with a highest value of 55% at 400 nm. The IPCE values of **XS19** based DSSCs with CDCA as coadsorbent showed improvement than that without CDCA, implying the dye aggregation on the surface of TiO_2 film. Unfortunately, the IPCE values for the three dyes were modest, and resulted in low short-circuit photocurrent density.

Figure 6 shows the I - V curves for DSSCs based on **XS17–19**. The light-to-electricity conversion efficiency (η) of the DSSCs under white-light irradiation can be calculated from the short-circuit photocurrent density (J_{sc}), the open-circuit photovoltage (V_{oc}), the fill factor of the cell (ff): $\eta = J_{\text{sc}} \times V_{\text{oc}} \times ff$.^{6c} The main photovoltaic parameters are listed in Table 2. The DSSCs based on **XS17** with 3 mmol/L CDCA as coadsorbent gave a J_{sc} of 3.7 mA/cm^2 , an open circuit voltage of 550 mV, and a fill factor of 0.68, corresponding to an overall conversion efficiency of 1.4%. Under the same conditions, the **XS19** sensitized cell yields a η of 1.3%. The photovoltaic performance of **XS17** is superior to that of **XS18–19**, which suggests that dye aggregations aroused by the increasing number of π bridges in turn decreased the photocurrent.

Possible reasons for the low IPCE and V_{oc} obtained for DSSCs based on **XS17–19** dyes are discussed as follows. From the Figure 2, it can be found that the electron density on the TiO_2 -binding oxygen in the

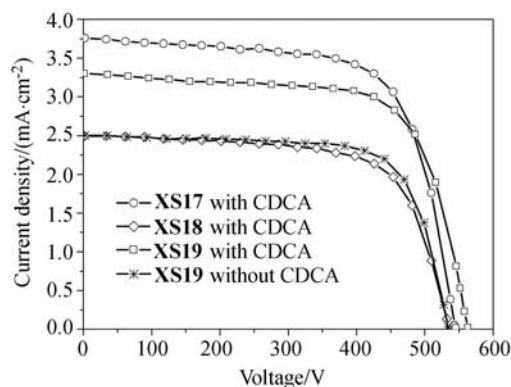


Figure 6 Current-potential (I - V) curves for the DSSCs based on **XS17**–**19** under AM 1.5 irradiation ($100 \text{ mW}\cdot\text{cm}^{-2}$).

Table 2 Photovoltaic performance of DSSCs sensitized with the four dyes^a

Dye	$J_{sc}/(\text{mA}\cdot\text{cm}^{-2})$	V_{oc}/mV	FF	$\eta/\%$
XS17	3.7	550	0.68	1.4
XS18	2.5	539	0.67	0.9
XS19	3.3	559	0.69	1.3
XS19^b	2.5	535	0.73	1.0
N719^b	12.3	711	0.68	6.2

^a Photovoltaic performances of DSSCs were measured under irradiation of AM 1.5 G simulated solar light ($100 \text{ mW}\cdot\text{cm}^{-2}$) at room temperature with a 0.16 cm^2 working area. The thickness of the TiO_2 film was $9 \mu\text{m}$. ^b Chenodeoxycholic acid (3 mmol/L) was not employed as co-adsorbate.

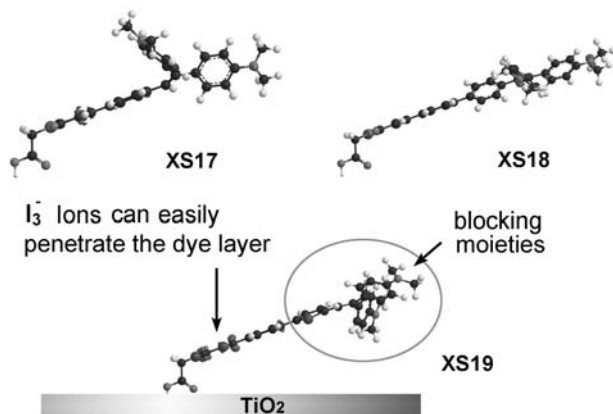


Figure 7 Graphical illustration of the geometries of the adsorbed dyes.

LUMO of **XS17**–**19** is negligible. This could result in lower electronic coupling between the dye and the semiconductor and, thereby, slower electron injection and also decrease the IPCE.³¹ On the other hand, the value of V_{oc} is dependent on the adsorption behavior of these dyes. As shown in Figure 7, the three dyes exhibit lying orientations on the TiO_2 surface. This adsorption geometry on TiO_2 leaves the π -conjugated system open to the electrolyte though bulky blocking moieties exhib-

iting. Therefore, I_3^- ions in electrolyte can easily penetrate the adsorbed dye layer, leading to fast electron recombination, and thus low photovoltages.³² In addition, the dye aggregation on the TiO_2 surface leading to self-quenching can be ignored for low conversion efficiency.^{7a}

Conclusion

A new class of 2D- π -A type organic dyes based on N,N -dimethylaryl amine for dye-sensitized solar cells is designed. The three dyes **XS17**–**19** show strong absorption bands at around 320–650 nm, and exhibit broad IPCE responses, suggesting that the N,N -dimethylaryl amine and diphenylvinyl moieties are effective unit for constructing photosensitizer. Unfortunately, devices based on **XS17**–**19** dyes gave low overall conversion efficiencies with modest IPCE and V_{oc} values, which mainly stem from the acceptor of rhodanine-3-acetic acid. Cell based on **XS17** gave a J_{sc} of $3.7 \text{ mA}/\text{cm}^2$, an open circuit voltage of 550 mV, and a fill factor of 0.68, corresponding to an overall conversion efficiency of 1.4%. Further optimization of chemical structure of N,N -dimethylaryl amine will be done in our next work.

Experimental

The FTO conducting glass (fluorine doped SnO_2 , sheet resistance $10 \Omega/\text{square}$, transmission $> 90\%$ in the visible) was obtained from Nippon Sheet Glass, Hyogo, Japan, and cleaned by a standard procedure. All reactions were conducted under nitrogen atmosphere in oven-dried glassware with magnetic stirring. Dichloromethane was dried and freshly distilled from calcium hydride under nitrogen atmosphere. Chromatographic purification was performed on silica gel (100–200 mesh) and analytical thin layer chromatography (TLC) on silica gel 60-F₂₅₄, which was detected by fluorescence. ^1H NMR (400 MHz) and ^{13}C NMR (100 MHz) spectra were measured with a Bruker AC 400 spectrometer using TMS as an internal standard. High resolution mass spectra were obtained with a Micromass GCT-TOF mass spectrometer. IR spectra were recorded as thin films or as solids in KBr pellets on a Perkin-Elmer FT210 spectrophotometer.

The absorption spectra of the dyes either in solution or on the adsorbed TiO_2 films were measured by HITACHI U-3310 spectrophotometer. Adsorption of the dye on the TiO_2 surface was done by soaking the TiO_2 electrode in a dry chloroform solution of the dye (standard concentration $3 \times 10^{-4} \text{ mol/L}$) at room temperature for 24 h. Fluorescence measurement was carried with a HITACHI F-4500 fluorescence spectrophotometer. FT-IR spectra were obtained with a Bio-Rad FTS 135 FT-IR instrument.

Electrochemical measurements were performed at room temperature under Ar atmosphere on a Voltammetric Analyzer (Metrohm, $\mu\text{Autolab III}$) with polymer

coated ITO glass as the working electrode, and platinum (Pt) plate as the counter electrode, using Ag/Ag⁺ (nonaqueous) electrode as reference electrode with a scan rate of 50 mV/s. Tetrabutylammonium perchlorate (TBAP, 0.1 mol/L) and acetonitrile were used as supporting electrolyte and solvent, respectively. The measurements were calibrated using ferrocene as standard. The redox potential of ferrocene internal reference was taken as 0.63 V vs. NHE.¹³ The solutions were purged with argon and stirred for 15 min before the measurements.

The photocurrent-voltage (*I-V*) characteristics of solar cells were carried out using a Keithley 2400 digital source meter controlled by a computer and a standard AM1.5 solar simulator-Oriel 91160—1000 (300 W) SOLAR SIMULATOR 2×2 BEAM. The active electrode area was 0.16 cm². The action spectra of monochromatic incident photon-to-current conversion efficiency (IPCE) for solar cells were performed by using a commercial setup (QTest Station 2000 IPCE Measurement System, CROWNTech, USA).

TiO₂ colloid was prepared according to the literature,³³ which was used for the preparation of the nanocrystalline films. The TiO₂ paste consisting of 18 wt% TiO₂, 9 wt% ethyl cellulose and 73 wt% terpineol was firstly prepared, which was printed on a conducting glass using a screen printing technique. The thickness of the TiO₂ film was controlled by selection of screen mesh size and repetition of printing. The film was dried in air at 120 °C for 30 min and calcined at 500 °C for 30 min under flowing oxygen before cooling to room temperature. The heated electrodes were impregnated with a 0.05 mol/L titanium tetrachloride solution in a water-saturated desiccator at 70 °C for 30 min and then recalcined at 500 °C for 30 min. The as-prepared TiO₂ electrode was stained by immersing it into a dye solution containing 300 μmol/L dye sensitizers and 3 mmol/L chenodeoxycholic acid (CDCA) in a mixture of chloroform and methanol (volume ratio 10/1) for 24 h. The CDCA was employed as a coadsorbate to prevent dye aggregations on the TiO₂ surface. Pt catalyst was deposited on the FTO glass by coating with a drop of H₂PtCl₆ solution (40 mmol/L in ethanol) with the heat treatment at 395 °C for 15 min to give photoanode. The photocathode (the dye-deposited TiO₂ film) was placed on top of the counter electrode and was tightly clipped together to form a cell. Electrolyte was then injected into the seam between two electrodes. The electrolyte employed was a solution of 0.6 mol/L 1,2-dimethyl-3-*n*-propylimidazolium iodide (DMPII), 0.1 mol/L LiI, 0.05 mol/L I₂, and 0.5 mol/L tertbutylpyridine in acetonitrile.

The detailed experimental procedures and characterization data

4-(2,2-Bis(4-(dimethylamino)phenyl)vinyl)benzaldehyde (2) A solution of compound **1** (421 mg, 1.0 mmol) in dry THF (10 mL) was cooled to -78 °C. To

this solution *n*-BuLi (0.42 mL, 2.7 mol/L in hexane, 1.134 mmol) was added dropwise through a dropping funnel. The mixture was stirred at this temperature for 2 h before DMF (0.32 mL, 4.0 mmol) dissolved in 10 mL of dry THF was added in a dropwise manner. The solution was allowed to warm to room temperature and stirred for 12 h. The reaction was quenched with saturated NH₄Cl, extracted with chloroform and dried over MgSO₄. After filtration and removal of the solvent under vacuum, the product was purified by a silica gel column [V(petroleum) : V(ethyl acetate)=3 : 1 as eluent] to give a yellow product (260 mg, 70% yield). m.p.: 178—180 °C; ¹H NMR (CDCl₃, 300 MHz) δ: 9.81 (s, 1H), 7.57 (d, *J*=8.4 Hz, 2H), 7.21 (d, *J*=8.7 Hz, 2H), 7.13 (d, *J*=8.4 Hz, 2H), 7.01 (d, *J*=8.7 Hz, 2H), 6.70 (s, 1H), 6.62 (d, *J*=8.7 Hz, 2H), 6.61 (d, *J*=8.7 Hz, 2H), 2.94 (s, 6H), 2.93 (s, 6H); ¹³C NMR (75 MHz, CDCl₃) δ: 191.8, 150.6, 150.2, 146.8, 145.7, 133.6, 131.6, 129.7, 129.6, 129.3, 127.8, 122.4, 112.3, 111.9, 40.5; IR (KBr) *v*: 3430, 3041, 2802, 2728, 1691, 1608, 1582 cm⁻¹; HRMS(EI) calcd for C₂₅H₂₆N₂O (M)⁺ 370.2045, found 370.2049.

(5-(1-(4-(2,2-Bis(4-dimethylamino-phenyl)-vinyl)-phenyl)-meth-ylidene)-4-oxo-2-thioxo-thiazolidin-3-yl) acetic acid (XS17) To a solution of compound **2** (279 mg, 0.75 mmol) and rhodamine-3-acetic acid (150 mg, 0.78 mmol) in absolute ethanol (15 mL) was added piperidine (50 μL). The solution was refluxed for 24 h. After cooling the solution, the solvent was removed *in vacuo*. The pure product was obtained by silica gel chromatography [V(CHCl₃) : V(MeOH)=10 : 1 as eluent] as a white powder (363 mg, 89% yield). m.p.: 153—154 °C; ¹H NMR (DMSO-*d*₆, 300 MHz) δ: 7.68 (s, 1H), 7.38 (d, *J*=8.4 Hz, 2H), 7.18—7.13 (m, 4H), 6.95 (d, *J*=8.7 Hz, 2H), 6.79 (s, 1H), 6.74—6.66 (m, 4H), 4.46 (s, 2H), 2.95 (s, 6H), 2.92 (s, 6H); ¹³C NMR (DMSO-*d*₆, 75 MHz) δ: 193.6, 167.7, 167.4, 150.9, 150.5, 146.1, 142.1, 133.2, 131.4, 131.2, 130.8, 130.3, 129.2, 127.5, 122.2, 121.6, 112.9, 112.4, 47.8, 44.2; IR (KBr) *v*: 3750, 3648, 2358, 2342, 1608, 1519 cm⁻¹; HRMS (ESI) calcd for C₃₀H₂₉N₃O₃S₂ (M+H)⁺ 544.1723, found 544.1731.

4'-(2,2-Bis(4-dimethylamino-phenyl)-vinyl)-bi-phenyl-4-carbaldehyde (4) A mixture of 4-bromobenzaldehyde (162 mg, 0.84 mmol), 4-(2,2-bis(4-(dimethylamino)phenyl)vinyl)phenylboronic acid (**3**) (216 mg, 0.56 mmol), Pd(PPh₃)₄ (50 mg, 0.042 mmol), aqueous 1 mol/L Na₂CO₃ (3 mL), and 10 mL DME was refluxed for 18 h under Ar. Ethyl acetate was added before cooling down to room temperature. The organic layer was separated and washed 3 times with water, dried over anhydrous MgSO₄, and filtered. After removing the solvent, the resulting solid was purified by column chromatography on silica gel (petroleum : ethyl acetate=10 : 1 as eluent) as a yellow powder (332 mg, 62 % yield). m.p.: 114—116 °C; ¹H NMR (CDCl₃, 400 MHz) δ: 10.03 (s, 1H), 7.72 (d, *J*=8.4 Hz, 2H), 7.44 (d, *J*=8.4 Hz, 2H), 7.27 (d, *J*=8.4 Hz, 2H), 7.18 (d, *J*=

8.4 Hz, 2H), 7.12—7.10 (m, 4H), 6.78 (s, 1H), 6.70 (d, $J=8.4$ Hz, 2H), 6.68 (d, $J=8.4$ Hz, 2H), 3.00 (s, 6H), 2.98 (s, 6H); ^{13}C NMR (CDCl_3 , 100 MHz) δ : 191.9, 150.3, 149.9, 147.1, 144.1, 139.4, 136.4, 134.9, 132.2, 131.5, 130.3, 129.9, 128.9, 128.4, 127.2, 126.8, 122.9, 112.4, 112.0, 40.6; IR (KBr) ν : 3449, 3072, 3027, 2952, 2801, 1698, 1607, 1590 cm^{-1} ; HRMS (EI) calcd for $\text{C}_{31}\text{H}_{30}\text{N}_2\text{O}$ (M^+) 446.2358, found 446.2361.

(5-(1-(4-(2,2-Bis(4-dimethylamino-phenyl)vinyl)-phenyl)-methylidene)-4-oxo-2-thioxo-thiazolidin-3-yl)-acetic acid (XS18) The product was synthesized according to the procedure for synthesis of **XS17**, giving a wine powder of the product in 65% yield. m.p.: 165—168 °C; ^1H NMR ($\text{DMSO}-d_6$, 300 MHz) δ : 7.90 (s, 1H), 7.85 (d, $J=8.4$ Hz, 2H), 7.69 (d, $J=8.7$ Hz, 2H), 7.56 (d, $J=8.4$ Hz, 2H), 7.18—7.14 (m, 4H), 6.96 (d, $J=8.4$ Hz, 2H), 6.80—6.66 (m, 5H), 4.71 (s, 2H), 2.94 (s, 6H), 2.91 (m, 6H); ^{13}C NMR ($\text{DMSO}-d_6$, 75 MHz) δ : 193.7, 167.9, 167.1, 150.7, 150.3, 143.9, 142.6, 139.3, 136.1, 134.2, 134.1, 132.2, 132.1, 131.6, 131.3, 130.2, 128.9, 128.0, 122.7, 121.9, 112.9, 112.5, 45.8, 40.6; IR (KBr) ν : 3674, 3545, 2358, 2342, 1558, 1507 cm^{-1} ; HRMS (ESI) calcd for $\text{C}_{36}\text{H}_{33}\text{N}_3\text{O}_3\text{S}_2$ ($\text{M}+\text{H}$) $^+$ 620.2036, found 620.2031.

4-(1-(4-(dimethylamino)phenyl)-2-(thiophen-2-yl)vinyl)-*N,N*-dimethylbenzenamine (6) To a suspension of diethyl bis(4-(dimethylamino) phenyl) methylphosphonate (**5**) (1.5 g, 3.6 mmol) in 20 mL dry THF at 0 °C under Ar, *t*-BuOK (600 mg, 5.4 mmol) was added and the mixture turned yellow. The mixture was stirred at this temperature for 1 h before thiophene-2-carbaldehyde (336 mg, 3 mmol) dissolved in 10 mL dry THF was added dropwise. The mixture was stirred at 0 °C for 1 h and moved into room temperature for another 12 h. Saturated NH_4Cl was added and the resulting mixture was extracted with EtOAc (20 mL \times 3). The combined extracts were washed with water and dried over MgSO_4 . After filtration and removal of the solvent under vacuum, the crude product was purified by column chromatography to give a yellow product in 44% yield. m.p.: 147—149 °C; ^1H NMR (CDCl_3 , 300 MHz) δ : 7.26—7.23 (m, 2H), 7.13—7.10 (m, 3H), 6.96—6.95 (m, 1H), 6.90—6.89 (m, 1H), 6.86—6.79 (m, 3H), 6.65 (d, $J=5.1$ Hz, 2H), 3.02 (s, 6H), 2.94 (s, 6H); ^{13}C NMR (CDCl_3 , 75 MHz) δ : 150.5, 150.1, 143.1, 140.7, 131.5, 131.2, 128.1, 127.7, 126.2, 125.0, 117.4, 113.1, 112.3, 40.8; IR (KBr) ν : 3800, 3566, 2359, 1610, 1521, 1352 cm^{-1} ; HRMS (ESI) calcd for $\text{C}_{22}\text{H}_{24}\text{N}_2\text{S}$ ($\text{M}+\text{H}$) $^+$ 349.1733, found 349.1728.

4-(5-(2,2-Bis(4-(dimethylamino)phenyl)vinyl)-thiophen-2-yl)benzaldehyde (7) Compound **6** (696 mg, 2 mmol) and NBS (356 mg, 2 mmol) were dissolved in DMF (100 mL) and stirred at room temperature for 24 h. The mixture was poured into water (100 mL), leading to a precipitate yellow solid. The precipitate was filtered and removal of the solvent under vacuum gave a yellow powder. The powder was not further purified and immediately used to react with

4-formylphenyl-boronic acid according to the procedure for compound **4**, giving an orange powder of the product (289 mg, 32% yield). m.p.: 103—104 °C; ^1H NMR (CDCl_3 , 400 MHz) δ : 9.96 (s, 1H), 7.81 (d, $J=8.4$ Hz, 2H), 7.58 (d, $J=8.4$ Hz, 2H), 7.29—7.25 (m, 3H), 7.17 (d, $J=8.4$ Hz, 2H), 7.09 (s, 1H), 6.90—6.85 (m, 3H), 6.69 (d, $J=8.8$ Hz, 2H), 3.07 (s, 6H), 2.99 (s, 6H); ^{13}C NMR (CDCl_3 , 100 MHz) δ : 40.4, 40.6, 112.0, 113.0, 116.6, 124.6, 125.4, 128.6, 130.3, 130.7, 131.1, 134.5, 140.5, 140.6, 142.4, 145.1, 150.1, 150.6, 191.3; IR (KBr) ν : 3764, 3648, 2358, 1700, 1597, 1520, 1336, 1201, 817 cm^{-1} ; HRMS (ESI) calcd for $\text{C}_{29}\text{H}_{28}\text{N}_2\text{OS}$ ($\text{M}+\text{H}$) $^+$ 453.1995, found 453.1990.

(5-(1-(4-(5-(2,2-Bis(4-dimethylamino-phenyl)-vinyl)-thiophen-2-yl)-phenyl)-methylidene)-4-oxo-2-thioxo-thiazolidin-3-yl)-acetic acid (XS19) The product was synthesized according to the procedure for synthesis of **XS17**, giving a wine powder of the product in 81% yield. m.p.: 168—170 °C; ^1H NMR ($\text{DMSO}-d_6$, 400 MHz) δ : 7.70—7.30 (m, 6H), 7.16—7.13 (m, 4H), 7.01—6.99 (m, 3H), 6.85 (d, $J=8.4$ Hz, 2H), 6.66 (d, $J=8.4$ Hz, 2H), 4.43 (s, 2H), 2.99 (s, 6H), 2.91 (s, 6H); ^{13}C NMR ($\text{DMSO}-d_6$, 100 MHz) δ : 193.4, 169.1, 167.3, 150.8, 150.4, 144.3, 141.9, 140.5, 136.5, 134.7, 131.9, 131.1, 130.0, 129.9, 128.2, 128.0, 126.7, 125.8, 122.2, 121.2, 113.3, 112.4, 46.6, 44.0; IR (KBr) ν : 3734, 3648, 2358, 2342, 1608, 1558 cm^{-1} ; HRMS (ESI) calcd for $\text{C}_{34}\text{H}_{31}\text{N}_3\text{O}_3\text{S}_3$ ($\text{M}-\text{H}$) $^+$ 624.1580, found 624.1589.

References

- Nazeeruddin, M. K.; Kay, A.; Rodicio, I.; Humphry-Baker, R.; Muller, E.; Liska, P.; Vlachopoulos, N.; Grätzel, M. *J. Am. Chem. Soc.* **1993**, *115*, 6382.
- Nazeeruddin, M. K.; Zakeeruddin, S. M.; Humphry-Baker, R.; Jirousek, M.; Liska, P.; Vlachopoulos, N.; Shklover, V.; Fischer, C.-H.; Grätzel, M. *Inorg. Chem.* **1999**, *38*, 6298.
- Nazeeruddin, M. K.; Péchy, P.; Renouard, T.; Zakeeruddin, S. M.; Humphry-Baker, R.; Comte, P.; Liska, P.; Cevey, L.; Costa, E.; Shklover, V.; Spiccia, L.; Deacon, G. B.; Bignozzi, C. A.; Grätzel, M. *J. Am. Chem. Soc.* **2001**, *123*, 1613.
- (a) Hara, K.; Sato, T.; Katoh, R.; Furube, A.; Ohga, Y.; Shinpo, A.; Suga, S.; Sayama, K.; Sugihara, H.; Arakawa, H. *J. Phys. Chem. B* **2003**, *107*, 509.
(b) Hara, K.; Kurashige, M.; Dan-oh, Y.; Kasada, C.; Shinpo, A.; Suga, S.; Sayama, K.; Arakawa, H. *New J. Chem.* **2003**, *27*, 783.
(c) Hara, K.; Sayama, K.; Ohga, Y.; Shinpo, A.; Suga, S.; Arakawa, H. *Chem. Commun.* **2001**, 569.
- (a) Wang, Z.; Cui, Y.; Hara, K. *Adv. Mater.* **2007**, *19*, 1.
(b) Hagberg, D. P.; Edvinsson, T.; Marinado, T.; Boschloo, G.; Hagfeldt, A.; Sun, L. *Chem. Commun.* **2006**, 2245.
(c) Shibano, Y.; Umeyama, T.; Matano, Y.; Imahori, H. *Org. Lett.* **2007**, *9*, 1971.
(d) Jung, I.; Lee, J. K.; Song, K.; Kang, S. O.; Ko, J. *J. Org. Chem.* **2007**, *72*, 3652.
(d) Kim, S.; Lee, J. K.; Kang, S. O.; Ko, J.; Yum, J.-H.;

- Fantacci, S.; De Angelis, F.; Di Censo, D.; Nazeeruddin, M. K.; Grätzel, M. *J. Am. Chem. Soc.* **2006**, *128*, 16701.
- (f) Kim, D.; Lee, J. K.; Kang, S. O.; Ko, J. *Tetrahedron* **2007**, *63*, 1913.
- (g) Choi, H.; Lee, J. K.; Song, K.; Kang, S. O.; Ko, J. *Tetrahedron* **2007**, *63*, 3115.
- 6 (a) Chen, Y. S.; Li, C.; Zeng, Z. H.; Wang, W. B.; Wang, X. S.; Zhang, B. W. *J. Mater. Chem.* **2005**, *15*, 1654.
- (b) Ehret, A.; Stuhl, L.; Spittler, M. T. *J. Phys. Chem.* **2001**, *105*, 9960.
- (c) Chen, X. Y.; Guo, J. H.; Peng, X. J.; Guo, M.; Xu, Y. Q.; Shi, L.; Liang, C. H.; Wang, L.; Gao, Y. L.; Sun, S. G.; Cai, S. M. *J. Photochem. Photobiol. A* **2005**, *171*, 231.
- (d) Cherepy, N. J.; Smestad, G. P.; Grätzel, M.; Zhang, J. Z. *J. Phys. Chem. B* **1997**, *101*, 9342.
- (e) Guo, M.; Diao, P.; Ren, Y. J.; Meng, F. S.; Tian, H.; Cai, S. M. *Sol. Energy Mater. Sol. Cells* **2005**, *88*, 23.
- 7 (a) Choi, H.; Baik, C.; Kang, S. O.; Ko, J.; Kang, M.-S.; Nazeeruddin, M. K.; Grätzel, M. *Angew. Chem., Int. Ed.* **2008**, *47*, 327.
- (b) Chang, Y. J.; Chow, T. J. *Tetrahedron* **2009**, *65*, 9626.
- 8 (a) Ning, Z. J.; Tian, H. *Chem. Commun.* **2009**, 5483.
- (b) Wu, W. J.; Meng, F. S.; Li, J.; Teng, X.; Hua, J. L. *Synth. Met.* **2009**, *159*, 1028.
- (c) Baik, C.; Kim, D.; Kang, M. S.; Song, K.; Kang, S. O.; Ko, J. *Tetrahedron* **2009**, *65*, 5302.
- (d) Liu, B.; Zhu, W.; Zhang, Q.; Wu, W.; Xu, M.; Ning, Z.; Xie, Y.; Tian, H. *Chem. Commun.* **2009**, 1766.
- 9 Li, G.; Zhou, Y. F.; Cao, X. B.; Bao, P.; Jiang, K. J.; Lin, Y.; Yang, L. M. *Chem. Commun.* **2009**, 2201.
- 10 (a) Wang, Z. S.; Li, F. Y.; Huang, C. H.; Wang, L.; Wei, M.; Jin, L. P.; Li, N. Q. *J. Phys. Chem. B* **2000**, *104*, 9676.
- (b) Yao, Q. H.; Meng, F. S.; Li, F. Y.; Tian, H.; Huang, C. H. *J. Mater. Chem.* **2003**, *13*, 1048.
- (c) Chen, R. K.; Yang, X. C.; Tian, H. N.; Wang, X. N. Hagfeldt, A.; Sun, L. C. *Chem. Mater.* **2007**, *19*, 4007.
- 11 Liang, M.; Xu, W.; Cai, F. S.; Chen, P. Q.; Peng, B.; Chen, J.; Li, Z. M. *J. Phys. Chem. C* **2007**, *111*, 4465.
- 12 Ning, Z. J.; Zhang, Q.; Wu, W. J.; Pei, H. C.; Liu, B.; Tian, H. *J. Org. Chem.* **2008**, *73*, 3791.
- 13 Hagberg, D. P.; Yum, J.-H.; Lee, H.; Angelis, F. D.; Marinado, T.; Karlsson, K. M.; Humphry-Baker, R.; Sun, L. C.; Hagfeldt, A.; Grätzel, M.; Nazeeruddin, M. K. *J. Am. Chem. Soc.* **2008**, *130*, 6259.
- 14 Zhang, G.; Bala, H.; Cheng, Y.; Shi, D.; Lv, X.; Yu, Q.; Wang, P. *Chem. Commun.* **2009**, 2198.
- 15 Zhang, F.; Luo, Y. H.; Song, J.-S.; Guo, X. Z.; Liu, W. L.; Ma, C. P.; Huang, Y.; Ge, M. F.; Bo, Z. S.; Meng, Q. B. *Dyes and Pigments* **2009**, *81*, 224.
- 16 (a) Ma, X.; Wu, W.; Zhang, Q.; Guo, F.; Meng, F.; Hua, J. *Dyes and Pigments* **2009**, *82*, 353.
- (b) Shen, P.; Liu, Y.; Huang, X.; Zhao, B.; Xiang, N.; Fei, J.; Liu, L.; Wang, X.; Huang, H.; Tan, S. *Dyes and Pigments* **2009**, *83*, 187.
- 17 Chen, H. J.; Huang, H.; Huang, X. W.; Clifford, J. N.; Forneli, A.; Palomares, E.; Zheng, X.-Y.; Zheng, L. P.; Wang, X. Y.; Shen, P.; Zhao, B.; Tan, S. T. *J. Phys. Chem. C* **2010**, *114*, 3280.
- 18 Li, Q. Q.; Lu, L. L.; Zhong, C.; Shi, J.; Huang, Q.; Jin, X. B.; Peng, T. Y.; Qin, J. G.; Li, Z. *J. Phys. Chem. B* **2009**, *113*, 14588.
- 19 Yang, Y.; Zhang, J.; Zhou, C. H.; Wu, S. J.; Xu, S.; Liu, W.; Han, H. W.; Chen, B. L.; Zhao, X. Z. *J. Phys. Chem. B* **2008**, *112*, 6594.
- 20 Cao, Y. M.; Bai, Y.; Yu, Q. J.; Cheng, Y. M.; Liu, S.; Shi, D.; Gao, F. F.; Wang, P. *J. Phys. Chem. C* **2009**, *113*, 6290.
- 21 Hara, K.; Kurashige, M.; Ito, S.; Shinpo, A.; Suga, S.; Sayama, K.; Arakawa, H. *Chem. Commun.* **2003**, 252.
- 22 Hara, K.; Sato, T.; Katoh, R.; Furube, A.; Yoshihara, T.; Murai, M.; Kurashige, M.; Ito, S.; Shinpo, A.; Suga, S.; Arakawa, H. *Adv. Funct. Mater.* **2005**, *15*, 246.
- 23 Kitamura, T.; Ikeda, M.; Shigaki, K.; Inoue, T.; Anderson, N. A.; Ai, X.; Lian, T.; Yanagida, S. *Chem. Mater.* **2004**, *16*, 1806.
- 24 (a) Horiuchi, T.; Miura, H.; Uchida, S. *Chem. Commun.* **2003**, 3036.
- (b) Horiuchi, T.; Miura, H.; Sumioka, K.; Uchida, S. *J. Am. Chem. Soc.* **2004**, *126*, 12218.
- 25 Pei, J.; Peng, S. J.; Shi, J. F.; Liang, Y. L.; Tao, Z. L.; Liang, J.; Chen, J. *J. Power Sources* **2009**, *187*, 620.
- 26 Roquet, S.; Cravino, A.; Leriche, P.; Alévêque, O.; Frère, P.; Roncali, J. *J. Am. Chem. Soc.* **2006**, *128*, 3459.
- 27 Xu, M.; Wenger, S.; Bara, H.; Shi, D.; Li, R.; Zhou, Y.; Zakeeruddin, S. M.; Grätzel, M.; Wang, P. *J. Phys. Chem. C* **2009**, *113*, 2966.
- 28 Thomas, K. R. J.; Hsu, Y. C.; Lin, J. T.; Lee, K. M.; Ho, K. C.; Lai, C. H.; Cheng, Y. M.; Chou, P. T. *Chem. Mater.* **2008**, *20*, 1830.
- 29 Hagfeldt, A.; Grätzel, M. *Chem. Rev.* **1995**, *95*, 49.
- 30 Tian, H.; Yang, X.; Chen, R.; Pan, Y.; Li, L.; Hagfeldt, A.; Sun, L. C. *Chem. Commun.* **2007**, 3741.
- 31 Wiberg, J.; Marinado, T.; Hagberg, D. P.; Sun, L. C.; Hagfeldt, A.; Albinsson, B. *J. Phys. Chem. C* **2009**, *113*, 3881.
- 32 Liang, Y.; Peng, B.; Chen, J. *J. Phys. Chem. C* **2010**, *114*, 10992.
- 33 Ito, S.; Murakami, T. N.; Comte, P.; Liska, P.; Grätzel, C.; Nazeeruddin, M. K.; Grätzel, M. *Thin Solid Films* **2008**, *516*, 4613.

(E1006295 Lu, Y.)